RSC Advances

Journal Name

ARTICLE

# Preparation of stable Bismuth Phosphate nanoparticles in phosphate glass and its magneto-optical study

`Received 00th January 20xx,
Accepted 00th January 20xx

DOI: 10.1039/x0xx00000x

www.rsc.org/

Jalindar D. Ambekar[a, b], Rajendra P. Panmand[a], Ravindra S. Sonawane[a], Sanjay K. Apte[a], Dilip G. Hundiwale[b], Bharat B. Kale [a] *

Herein, synthesis of Bismuth Phospahate ($BiPO_4$) nanocrystals in low melting phosphate glass and its optical and magneto-optical properties has been investigated. The presence of $BiPO_4$ nanoparticles are confirmed by X-ray diffractometer and Raman spectrometer. The optical transmission spectra of the glass samples showed that red shift in absorption edge is due to the presence of $BiPO_4$ nanoparticles in glass. Faraday rotation tests on the glass nanocomposite shows giant enhancement in verdet constant due to $BiPO_4$ nanoparticles in phosphate glass. The $BiPO_4$ - glass nanosystem showed higher verdet constant (21.2deg / T-cm) which shows 3 fold significant enhancement in the verdet constant of BK-7 glass(7.52 deg / T-cm). The novel $BiPO_4$ glass nanocomposite may have potential application in magneto optical devices.

## Introduction

The glass is a supercooled liquid which is transparent and amorphous in nature. Glasses are the fusion of inorganic compounds which are cooled to a rigid condition without any crystallization. The main distinction between crystalline solid and glasses is the presence of long-range ordered crystal structure while short range orders (random) in glasses[1a]. The optimization of properties which are function of composition and other processing parameters requires a good knowledge of the microscopic glassy structure[1b].

In the recent years, glasses with the nanoparticles dispersed systems (NDS`s) and optically functional nanoparticles embedded in glass matrices have attracted the researcher in the field of the applied optics such as light-emitting diodes, optical switches, and optical circuits.[1c,2] NDS can be used in the magneto-optical devices such as an optical isolator and an optical modulator. [3,4,5a,5b,5c] Magneto-optic glasses have applications in Magneto-Optic Current transformers (MOCTs), Optical fibre sensors and highly sensitive magnetic field detectors.[6] Optical current sensors have significant applications in high voltage environments due to their immunity to Electromagnetic Induction (EMI) and high bandwidth capabilities[7]. Highly sensitive magnetic field sensors can be very useful in detecting current less than milli-ampere. Sensitivity and linearity of existing magneto-optic devices are the limiting parameters which necessitate further research on enhancement of magneto-optic effect in glasses.

Faraday Rotation (FR) properties of glasses have been extensively studied over the last few years. A major part of these studies was on investigations of the magneto-optical properties of binary and ternary glass system activated due to doped rare earth ions[8]. The FR properties of silica based glasses have been extensively studied over last few years[9-11a]. However, very limited study has been carried out on FR properties of phosphate glasses[11b]. The melting temperature of silica based glasses is in the range of 1300-1500$^0$C which is more energy intensive and quite critical to cast the blank at this temperature. In order to overcome these problems, researchers have focused their attention on the synthesis and characterization of low temperature melting glasses such as phosphate glasses. Phosphate glasses are known for their unique properties viz. high thermal expansion, low melting temperature, low refractive index and greater ultraviolet transparency etc. These properties, lead their application as glass-to-metals seals and in different optical devices[12-16.] However, phosphate glasses are less used commercially due to their poor chemical solubility[17,18]. In view of this, we have attempted the fabrication of stable phosphate glass. The present paper reports the synthesis of $BiPO_4$ phosphate glasses and its magneto-optical properties. The magneto optical properties are the measure of Faraday rotation. The Verdet constant is calculated from the Faraday rotation. The Faraday effect i.e. diamagnetic and paramagnetic effect is already well-known for glasses. The theoretical explanation of Faraday Effect with respect to the birefringence is given as follow.

[a.] Centre For Materials For Electronics Technology (C-MET), Panchawati, Off Pashan Road, Pune, 411 008. INDIA *bbkale1@gmail.com
[b.] School of Chemical Sciences, North Maharashtra University, Jalgaon, 425001, INDIA
† Footnotes relating to the title and/or authors should appear here.
Electronic Supplementary Information (ESI) available: [details of any supplementary information available should be included here]. See DOI: 10.1039/x0xx00000x

**Photo-elastic Modulation technique of Faraday rotation measurements**

If x is the direction assigned to the polarization of incident light, then the wave coming out of the sample after rotation by an angle θ can be expressed as

$\bar{E} = E_0(cos\theta\hat{x} + sin\theta\hat{y})$ ------------ (1)

The light travels through the Photo-Elastic Modulator (PEM), which imposes a sinusoidal oscillation in the polarization angle. If the PEM modulation amplitude is $A_o$ and frequency is Ω, then the resultant wave field is

$$\bar{E} = E_0(cos\theta e^{i\frac{A}{2}}\hat{x} + sin\theta e^{-i\frac{A}{2}}\hat{y})$$

where$A=A_o\cos\Omega t$

The polarization oriented at 45° with respect to the x axis then allows the measurements of the original polarization angle.

$$\bar{E}_{det.} = \frac{1}{\sqrt{2}}(\hat{x} + \hat{y}).\left[E_0(cos\theta e^{i\frac{A}{2}}\hat{x} + sin\theta e^{-i\frac{A}{2}}\hat{y})\right](\frac{1}{\sqrt{2}}(\hat{x} + \hat{y}))$$

$$\bar{E}_{det.} = \frac{1}{2}\left[E_0(cos\theta e^{i\frac{A}{2}} + sin\theta e^{-i\frac{A}{2}})\right](\hat{x} + \hat{y}))$$

Power at the detector is given by

$$P_{det.} = |E_{det}|^2 = \frac{E_o}{2}(1 + \sin 2\theta \cos A)$$

This Expression can be expanded in the Bessel function coefficient:

$$P_{det.} = \frac{E_o}{2}(1 + \sin 2\theta \cos(A_0 cos\Omega t))$$

$$P_{det.} \approx \frac{E_o}{2}(1 + J_0(A_o)\sin 2\theta + 2\, J_2(A_0)\sin 2\theta \cos 2\Omega t)$$

By choosing modulation amplitude which is zero of the lowest order Bessel functions, and measuring both the static signal and second harmonic of the modulation frequency, we can extract the polarization angle. The zero of the Bessel function is 0.383 waves (2.405 rad), which eliminates the second term of the above equation. Signals from the detector can be written as the DC term and term that oscillate at the second harmonics of the PEM modulation, whose amplitude is referred as $V_{2f}$. In volts this signal is expressed as:

$$V_{det.} = V_{DC} + V_{2f}\cos 2\Omega t = \frac{E_o}{2}(1 + 2\, J_2(A_0)\sin(2\theta)\cos 2\Omega t)$$

We can deduct the Faraday angle by measuring each of these signals independently. It is assumed that the Faraday angle is very small and factor $\sqrt{2}$ in introduced to account the RMS read by Lock in Amplifier.

$$\frac{V_{2f}}{\sqrt{2}V_{DC}} = 2J_2(2.405)2\theta = 4\,(0.2499)\theta$$

$$\theta = \frac{93.8\, V_{2f}}{\sqrt{2}V_{DC}}$$

In the present communication, considering the potential of nanocrystalline glasses, we have developed quantum dots of Bismuth phosphate in stable phosphate glasses. This nanocrystalline glass has been characterized thoroughly to investigate structural and optical properties. The Faraday rotations were measure with magnetic field to investigate magneto-optical properties. The glasses with $BiPO_4$ nanocrystals show good magneto-optical properties which are hitherto unattempted.

## Experimental

**Preparations of glasses**

The raw materials for host glass and $BiPO_4$ glass nanocomposite with their composition: 66 wt % $P_2O_5$, 20 wt % $K_2O$, 10 wt % $B_2O_3$, 4 wt % $Ta_2O_5$ and 66 wt % $P_2O_5$, 20 wt % $Bi_2O_3$, 8wt % $K_2O$, 5 wt % $B_2O_3$, 1 wt % $Ta_2O_5$ of 99-99.9% purity were procured from reputed firm like Aldrich. All the chemicals were used as received.

The host glass and $BiPO_4$ nanoparticles in phosphate glasses were prepared by thoroughly mixing and melting appropriate amount of analytical reagent grade of all chemicals. The well-mixed all above chemicals were preheated slowly to 450$^0$C, prior to melting in an alumina crucible to remove $H_2O$, $NH_3$, $CO_2$. The preheated mixture was melted at temperature in the range of 800-850°C in the alumina crucible. The melt obtained was soaked for 2 h, then crucible was removed from furnace and melt was air quenched on highly polished stainless steel preheated mould. The mould was preheated at ~400°C to prevent cracking of the glass because of the thermal shock. These glasses were annealed to room temperature at the cooling rate 0.5$^0$C/min.

**Characterization**

The glass samples prepared were characterized with the help of different characterization techniques. The crystalline phase and crystallite size was determined from X-ray powder diffraction (XRD) technique (XRD, Advance D8, Bruker-AXS). Room temperature micro Raman scattering (RS) was performed using a HR 800-Raman Spectroscopy, Horiba Jobin Yvon, France, with an excitation at 632.81nm by a coherent He-Ne ion laser and a liquid nitrogen cooled CCD detector to collect and process the backscattered data. Optical characterization of all the glass composites was performed using UV-Vis-NIR spectrophotometer (UV-Vis-NIR, Perkin-Elmer λ-950). The surface characterization of the glasses was performed using High Resolution Transmission Electron Microscope (HRTEM, JEOL, 2010F). For HRTEM studies, the glass samples were prepared by dispersing the glass powder in ethanol, followed by sonication in an ultrasonic bath for 10 min and then drop casting the sample on a carbon coated copper grid and by followed by drying.

**Experimental set up for measurement of Faraday rotation**

The experimental setup is shown in Fig. 2. Diode lasers ($\lambda_0$= 405, 532, 635, 670, 980, 1310nm) were used as the light source. Details of the experimental setup for the measurement of Verdet constant at relatively low fields of 2-4mT rms have been reported earlier[19,20]. The present experimental setup was based on these reports. Use of AC magnetic fields meant low fields could be generated at convenient levels to avoid excess heat from usage of bulky coils. Use of AC magnetic field method facilitates an efficient method of calculating the Verdet Constant by using the phase sensitive detection technique of the lock in amplifier and using a Fourier transform based method to compute the actual degree of rotation and hence the Verdet Constant. A Helmholtz coil capable of generating magnetic field upto 7mT rms was used. This ensured uniformity of the field. The coil was driven at 60Hz frequency. The optical chopper wheel pulsed light at a set frequency equal to that of the magnetic field frequency.

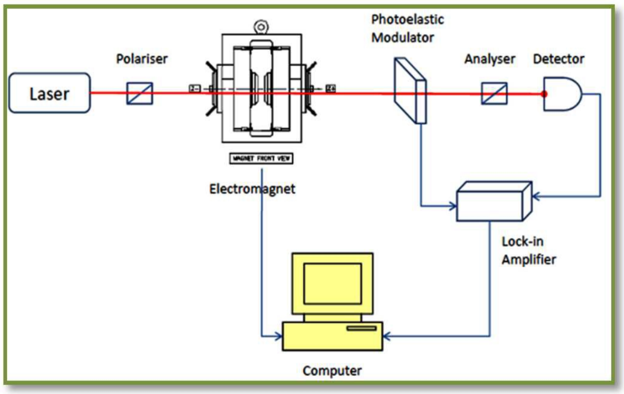


Figure1. Experimental Setup for Measuring Faraday rotation angle

A high speed photodetector from Thorlabs®, DET 100 was used to measure relatively small changes in intensity. The photodetector has a spectral response from 350-1100nm and was used to convert the light signal into an equivalent voltage output. A Phywe Tesla meter was used for the measurement of magnetic field. A National Instruments® data-logger data acquisition device was used in conjunction with LabVIEW® software to interface the output of the lock in amplifier to a computer in order to accurately record and maintain data. Initial measurements of Verdet constant on known magneto-optic glasses such as BK-7 and SF-57 in our setup yielded an accuracy of 6% when compared with published values. [19,21]

## Result & Discussion:

### X-Ray Diffraction analysis

X-ray diffractrometry of glass samples (Figure 2) gives evidence of growth of hexagonal bismuth phosphate ($BiPO_4$) nanocrystals in the matrix. (JCPDS data card No.15-0766). The broadening of peaks is induced by the small size of nanocrystals embedded in glass matrix. Average crystallite size was determined from XRD data using well-known Scherrer's formula and is observed to be 9-10 nm. The nanocrystal size calculated from the XRD is slightly higher than observed size and it may due to the nanoparticles are embedded in glassy matrix. The noisy peaks obtained are due to the insulating amorphous glass matrix. From XRD of host glass, it is also revealed that the as usual amorphous structure of the host glass.

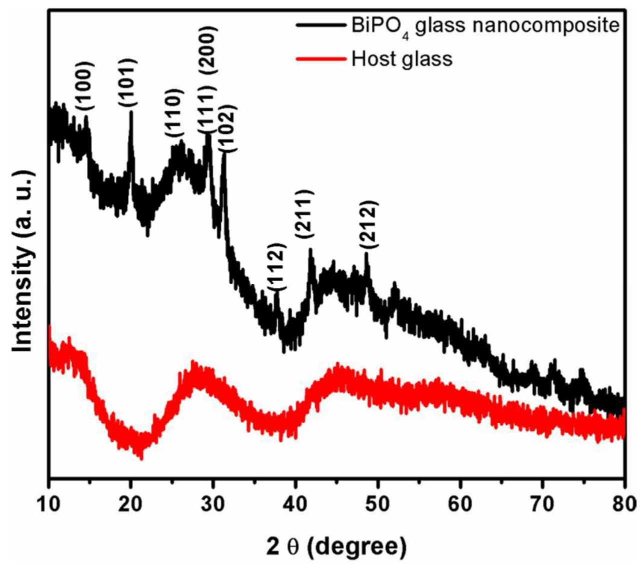


Figure 2.XRD of $BiPO_4$ nanoparticles in glass and host glass.

### Raman Spectroscopy

The $BiPO_4$ nanoparticles in glass nanocomposite were further characterized using Raman spectroscopy in the 100–1200 $cm^{-1}$ region (figure 3). All assigned peaks are summarized in table 1.Notably, the observed absorption bands in these spectra are in good agreement with the literature.[22a] The intense peak at 202 $cm^{-1}$ may be assigned to the symmetric bending vibration of Bi–O. One of the strong features of Raman spectroscopy is that, bands below 400$cm^{-1}$ can be readily determined. As a result, the intense bands attributable to M–O vibrations can be ascertained. Thus, the Raman bands between 450 and 600$cm^{-1}$ in the spectra in figure 3 were attributed to the $v_4$ bending modes of the $PO_4$ units and the two intense bands between 950 and 1062$cm^{-1}$ were ascribed to the $v_1$ symmetric and $v_3$ asymmetric stretching modes of the $PO_4$ tetrahedron. The additional peaks at 712 and 1130 $cm^{-1}$ were due to M-O-P symmetric stretching vibration and P-O stretching vibration (see figure 3).[22b,22c] It study shows the presence of $BiPO_4$ nanoparticles in glass matrix.

Table 1 : Summary of assigned Raman Peaks

| Sr. No | Peak frequency ($cm^{-1}$) | Peak assignments |
|---|---|---|
| 1 | 202 | An O-Bi-O symmetric bending mode |
| 2 | 400 | B-O vibrations and $v_2$ bending modes of $PO_4$ units |
| 3 | 446 and 600 | $v_4$ bending modes of the $PO_4$ |
| 4 | 712, 730 | M-O-P symmetric stretching vibration |
| 5 | 966 | $v_1$ symmetric stretching modes of the $PO_4$ tetrahedron |
| 6 | 1062 & 1130 | $v_3$ antisymmetric stretching modes of the $PO_4$ tetrahedron & P-O stretching vibration. |

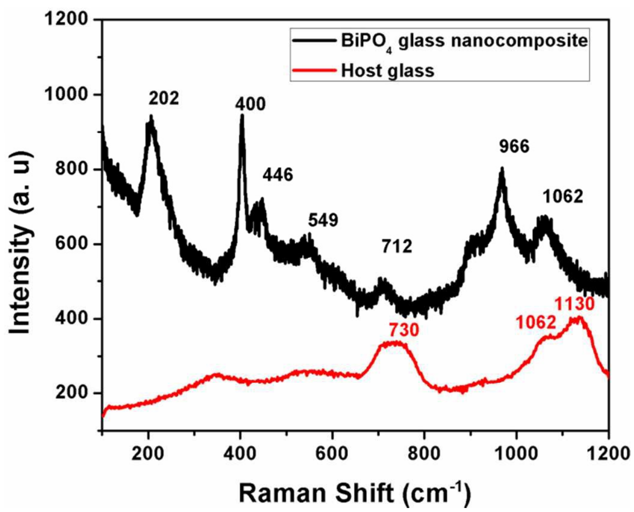


Figure 3.Raman spectra of $BiPO_4$ glass nanocomposite and host glass.

Figure S1 (see supporting information) shows the FT-IR spectrum of $BiPO_4$ glass nanocomposite in the range 600 to 2000 $cm^{-1}$. The broad peak observed at 1164 $cm^{-1}$ is due to O-P-O asymmetric stretching. While, 722 and 845 cm-1 are due to symmetric and asymmetric stretching of bridging oxygen (P-O-P).

**Transmission Electron Microscopy**

The glasses containing the $BiPO_4$ nanoparticles were characterized using TEM for morphological study of $BiPO_4$ nanoparticles into the glass matrix. Figure 2 shows a TEM images and Electron Diffraction (ED) pattern corresponding to $BiPO_4$ nanoparticles embedded in phosphate glass. TEM images clearly show the nanocrystalline phase in the glass.

From the TEM images (Fig. 4a and b), the particle size of $BiPO_4$ was observed in the range of 5 to 6 nm for the $BiPO_4$ glass nanocomposite. Figure 4c shows the High Resolution Transmission Electron Microscopic (HRTEM) image. HRTEM reveals that inter planer spacing is about 0.186 nm which is corresponds to (212) lattice planes of hexagonal $BiPO_4$ and it is supported by the XRD. Electron Diffraction pattern shows the polycrystalline nature of $BiPO_4$ nanoparticles. The XRD and ED pattern clearly shows the existence of $BiPO_4$ nanocrystals.

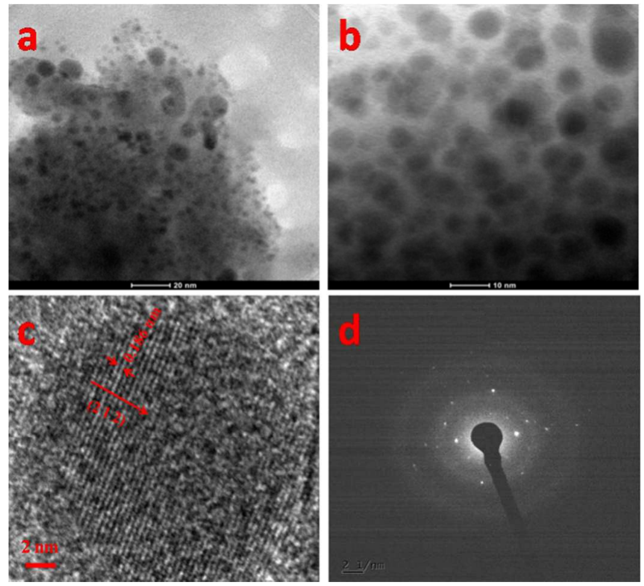


Figure 4.(a-c) TEM images and (d)Electron Diffraction (ED) pattern of $BiPO_4$ nanoparticles embedded in phosphate glass.

**Optical characterization**

The UV spectrum shows the optical transmission spectra of the glass nanosystem (figure 5).

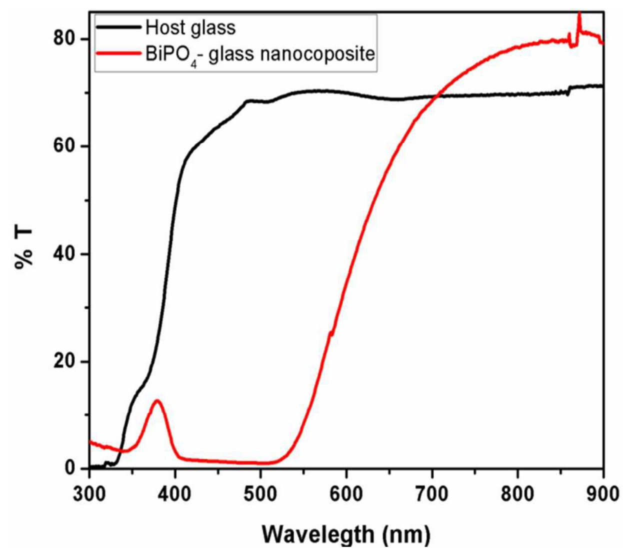


Figure 5. UV-Vis. Transmittance spectra of $BiPO_4$ glass nanocomposite.

From transmittance spectra (figure 5), it is concluded that the there is a strong red shift in absorption edge with introduction of $BiPO_4$ nanoparticles in glass matrix. Host glass shows the band gap 3.51 eV while $BiPO_4$ glass nanocomposite shows 2.04eV. Figure 6 shows the actual photographs of glasses with and without $BiPO_4$ nanoparticles in glass. It clearly shows that there is change in colour from dark orange to colourless.

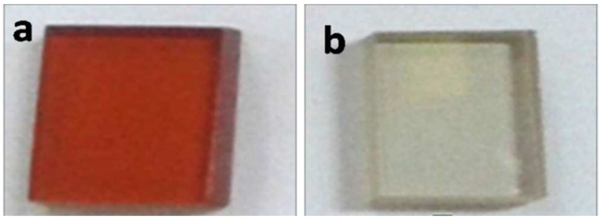


Figure 6. Actual photographs of the glasses. a: $BiPO_4$ glass nanocomposite, b: Host glass.

In the present study, FR was measured for the $BiPO_4$ -phosphate glass nanocomposite at room temperature. These glass nanocomposites were studied in the range of magnetic field 0-214mT, with a diode laser of different wavelengths. Averaging of the photo detector intensities was carried out at each value of the magnetic field for all nanocomposites. Normalization of relative change in intensities was done with respect to intensity of blank host sample. The FR angles were calculated from following equation:[23]

$$\theta_f = \frac{93.8}{1.414}\frac{V_{ref}}{V_{DC}}$$

Where $V_{ref}$ is the relative change in intensity and I is the intensity with the blank sample. Figure 7 shows the magnetic field dependant Faraday rotation (A-C) and wavelength dependant Verdet constant of $BiPO_4$ – glasses nanocomposite, host glass and BK-7 glass.

The quantum dot-glass nanocomposite demonstrated size related FR magnetic field strength. Figure 7 shows the linear increment of FR with magnetic field as expected and the variation in FR for $BiPO_4$ – glass nanocomposite, Host glass and BK-7 glass. The variation of the Verdet constant is shown in table 2 in details. There is a significant enhancement of FR in $BiPO_4$glass nanocomposite with respect to the host glass and standard BK-7 glass. $BiPO_4$ - Glass nanocomposite showed high verdet constant (21.2 $^0$/T cm) at 405 nm which are 2 and 3 times higher than the host glass and BK-7 glass, respectively. Surprisingly, the host glass itself showed high Verdet constant (9.64 $^0$/ T cm) compared to the earlier reported value. There is 68 times enhancement in the verdet constant for the $BiPO_4$ – glass nanocomposite as compared to the previous reported value (0.312$^0$ T/ cm).[24] This may be because of the higher refractive index of glass due to presence of $BiPO_4$. However, this unique observation is not fully understood yet, which require further discussion and study. We plan on investigating further the magnetic properties of the $BiPO_4$ –glasses nanocomposite while also pursuing femtosecond time-resolved photoluminescence studies to ultimately elucidate the origin of the large Faraday Effect in these materials.

Table 2.Verdet constant of $BiPO_4$ glass, host glass and BK-7 glass

| Wavelength (nm) | Verdet constant (degree/T-cm) | | |
|---|---|---|---|
| | $BiPO_4$ glass nanocomposite | host glass | BK-7 glass |
| Thickness (cm) | 0.27 | 0.31 | 1.80 |
| 405 | 21.2 | 9.64 | 7.52 |
| 532 | 8.7 | 4.96 | 3.65 |
| 635 | 6.4 | 1.01 | 2.61 |
| 670 | 7.1 | 1.56 | 2.54 |
| 980 | 2.3 | 0.75 | 1.13 |
| 1310 | 1.4 | 0.24 | 0.73 |

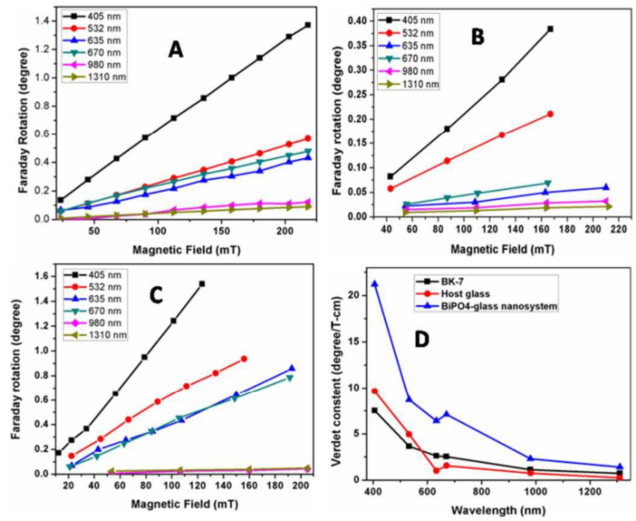


Figure 7.Magnetic field dependant Faraday rotation of A: $BiPO_4$ – glasses nanocomposite, B: Host glass and C: BK-7 glass. D: Wavelength dependant Verdet constant of $BiPO_4$ – glasses nanocomposite, host glass and BK-7 glass.

## Conclusions

A new, chemically stable host phosphate glass composition having low melting temperature i. e. 800-850$^0$C has been investigated. Bismuth Phosphate ($BiPO_4$) nanoparticles were embedded in the above newly developed phosphate glass. Effect of $BiPO_4$ content on the optical and magneto-optical properties has been investigated. From the UV-Vis spectra, it was observed that the optical cut-off of theses glasses was shifted to higher wavelength in presence of $BiPO_4$ nanoparticles. The nanoparticles of $BiPO_4$ were uniformly distributed in the glass matrix with average particle size of 5-6 nm. The highest verdet constant (21.2 $^0$/T cm) has been observed for glass nanocomposite with $BiPO_4$ nanoparticles which is higher than the host glass and standard BK-7 glass. This enhancement of verdet constant can be attributed to the increased excitonic confinement by the quantum dot grown in the glass matrix. This type of significant enhanced in Verdet constant for $BiPO_4$ phosphate glass nanocomposite is reported first time. The novel $BiPO_4$ quantum dot-glass nanocomposite may have potential application in magneto optical devices.

## Acknowledgements

Authors would like to thanks to Executive Director, C-MET for technical support and DeitY, New Delhi for financial support.

## Notes and references

1 (a) C. Gautam, A. K. Yadav, and A. K. Singh, *ISRN Ceramics*, 2012, 2012, 428497; (b) A. K. Yadav, C. R. Gautam, P. Singh, *RSC Adv*, 2015, **5**, 2819. (c) C. Inui, H. Kura, T. Sato, Y. Tsuge, S. Shiratori, H. Ohkita, A. Tagaya, and Y. Koike, *J. Mater. Sci.* 2007, **42**, 8144.
2 W. Caseri, *Macromol. Rapid Commun*. 2000, **21**, 705.
3 Y. A. Banakov, B. L. Scott, V. Golub, L. Kelly, V. Reddy, and K. L. Stokes, *J. Phys. Chem. Solids* 2004, **65**, 1055.
4 D. A. Smith, Y. A. Barnakov, B. L. Scott, S. A. White, and K. L. Stokes, *J. Appl. Phys.*2005, **97**, 10M504.
5 (a) Q. P. Chen, L. Wan, Q. L. Chen, M. Zhang, *Adv. Mater. Res.* 2011, **13**, 271; (b) R. P. Panmand, G. Kumar, S. M. Mahajan, M. V Kulkarni, D. P. Amalnerkar, Bharat B Kale, S. W. Gosavi, *J. of Appl. Phys*. 2011, **109**, 033101; (c) R. P. Panmand, G. Kumar, S. M. Mahajan, M. V. Kulkarni, B. B. Kale, S. W. Gosavi, *J. Mater. Chem. C*, 2013, **1**, 1203.
6 L. Sun, S. Jiang, J. R. Marciante, *Opt. Express,* 2010 **18,** 5408.
7 P. R. Watekar, H. Yang, S. Ju, W. T. Han, *Opt. Express,* 2009, **17**, 3157.
8 I. Edelman, J. Kliara, *phys. Status Solids A,* 2009, **246**, 2216.
9 T. Hayakawa, M Nogami, N. Sawanobori, *Chem. Mater*. 2002, **14**, 3223.
10 J. H. Kratzen and J. Schroeder, *J. Non-Cryst. Solids,* 2004, **349**, 299.
11 (a) P.I. Nikitin, *IEEE J. Quant. Electron*. 1965, **28**, 256; (b) S. N. Garaje, S. K. Apte, G. Kumar, R. P. Panmand, S. D. Naik, S. M. Mahajan, R. Chand, B. B. Kale, *Mater. Res. Bull*. 2013, **48,** 901.
12 M. Ivanda, K. Babocsi, C. Dem, M. Montagna, W. Kiefer, *phys. Rev. B,* 2003, **67,** 15.
13 A. Lipovskii, E. Kolobkova, V. petrikov, *Appl, phys. Lett*. 1997, **71**, 23.
14 P. Maly, T. Miyoshi, *J. Lumin***.** 1997, **90,** 1.
15 B. Vaynberg, M. matusovsky, M. Rosenbluh, E. Kolobkova, A. Lipovsii, *Opt. Commun.* 1996, **132**, 3.
16 H. S. Liu, T. S. Chin, S. W. Yung, *Mater. Chem. Phys*. 1997, **50,** 1.
17 D. Richard, P. Roussignol, C. Flytzanis, N. Neuroth, *Phys. A: Stat. Theor. Phys*. 1989, **157**, 91.
18 S. H. Risbud, *Thermochim. Acta,* 1996, **280,** 38.
19 A.Jain, J.Kumar, L. Li, F.Zhou and S.Tripathy, *Am. J. Phys*. 1999, **67**, 714.
20 K.Turvey, *Rev. Sci. Instrum*. 1993, **64**, 1561.
21 C. Liu, Y. Kon, J. Heo, *J. Non-Cryst. Solids*, 2006, **355**, 1880.
22 (a) L. W. Cheng, J. C. Tsai, T. Y. Huang, C. W. Huang, B. Unnikrishnan, Y. W. Lin, *Mater. Res. Express,* 2014, **1**, 025023; (b) M. R. Sahar, A. Wahab, M. A. Hussein, R. Hussin, *J. Non-Cryst. Solids*, 2007, **353**, 1134; (c) H. Takabe, Y. Baba, M. Kuwabara, *J. Non-Cryst. Solids*, 2006, **352**, 3088.
23 P. A. Williams, A. H. Rose G. W. Day, *Appl. Opt*., 1991, **30,** 1176.
24 G. Kumar, S. K. Apte, S. N. Garaje, M. V. Kulkarni, S. M. Mahajan, B.B. Kale, *Appl. Phys. A,* 2010, **98**, 531.



 

# Preparation of stable Bismuth Phosphate nanoparticles in phosphate glass and its magneto-optical study

*Jalindar D. Ambekar [a, b], Rajendra P. Panmand [a], Ravindra S. Sonawane [a], Sanjay K. Apte [a], Dilip G. Hundiwale [b], Bharat B. Kale [a] **

Herein, we have demonstrated the stable Bismuth Phospahate ($BiPO_4$) nanocrystals in low melting phosphate glass for magneto-optical Faraday rotation study.